Global Climate Change and Variability in State-Of-The-Art Models

S. Kravtsov[1], M. Wyatt[2], J. Curry[3] and A. Tsonis[1]

[1]University of Wisconsin-Milwaukee, Department of Mathematical Sciences, Atmospheric Sciences Group

[2]University of Colorado-Boulder [3]Georgia Tech, Atlanta, GA

UNIVERSITY of WISCONSIN UWMILWAUKEE College of Letters and Science ATMOSPHERIC SCIENCE DEPARTMENT OF MATHEMATICAL SCIENCES

Computational Sciences AT MARQUETTE UNIVERSITY

Introduction

State-of-the-art global coupled climate models used to simulate 20th century climate use similar dynamical cores, but differ in details of the forcing and in the parameterizations of unresolved subgrid-scale physical processes (Taylor et al. 2012). We consider 18 independent ensembles of these model simulations (**Table 1**) for attribution of the 20th century climate change.

Table 1: CMIP-5 twentieth century simulations with four or more realizations (18 ensembles with the total of 116 simulations).

Model #	Model acronym	Number of realizations	Aerosol indirect effects (cloud albedo+lifetime)
1.	CCSM4	6	
2.	CNRM-CM5	10	
3.	CSIRO-Mk3-6-0	10	Y
4.	CanESM2	5	
5.	GFDL-CM2p1	10	
6.	GFDL-CM3	5	Y
7.	GISS-E2-Hp1	6	
8.	GISS-E2-Hp2	5	
9.	GISS-E2-Hp3	6	
10.	GISS-E2-Rp1	6	
11.	GISS-E2-Rp2	6	
12.	GISS-E2-Rp3	6	
13.	GISS-E2-Rp4	6	
14.	HadCM3	10	
15.	HadGEM2-ES	5	Y
16.	IPSL-CM5A-LR	6	
17.	MIROC5	4	Y
18.	MRI-CGCM3	4	Y

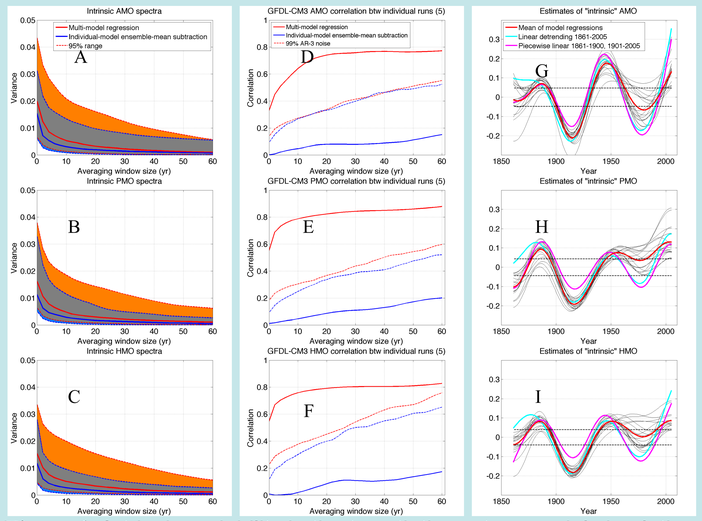

Figure 1: Intrinsic variability in the twentieth-century model simulations with four and more ensemble members identified using two different methods for estimating the forced signal — the multi-model regional regression method (method 1), and the classical subtraction of the individual-model ensemble mean (method 2). Left column: the spectra of intrinsic variability; these spectra plot the variance of the running-mean low-pass filtered time series of each climate index against the averaging window size. The dashed lines filled with color shading (see legend) show the 95% spread of the spectra across the total of 116 simulations considered. Middle column: the correlation measure of statistical independence between multiple realizations of the GFDL CM3 model. Low correlation measure indicates statistical independence. Dashed lines show the 99th percentile of the correlation measure based on the 1000 simulations of the corresponding AR-3 red-noise model. Right column: estimates of the observed multidecadal intrinsic variability. The semi-empirical estimates (thin black lines) were computed based on the forced signals obtained using method 2 for each of the 18 model ensembles considered, with heavy red line indicating the average over these individual estimates. Additional heavy lines are for results based on linear detrending. The distance between the black dashed lines in each plot shows the 95th percentile of the standard deviations for multidecadal intrinsic variability estimated using method 2 over the 116 simulations considered.

Forced-vs.-Intrinsic Variability

We concentrate on the behavior of surface temperature averaged over the North Atlantic (AMO), North Pacific (PMO) and the entire Northern Hemisphere (HMO) region (Steinman et al. 2015). The central issue here is attribution of the temperature evolution to a combination of externally forced (by variable CO_2 or aerosol concentrations, solar forcing etc.) and intrinsic climate variability (which can exist under the constant forcing). Two ways to isolate the two types of variability in a climate variable x are (Kravtsov and Spannagle 2008; Steinman et al. 2015)

$$x_k^{(n)} = \left[x^{(n)}\right] + \epsilon_k^{(n)}, \;\; x_k^{(n)} = a_k\left[x^{(n)}\right] + \epsilon_k^{(n)}, \qquad (1a,b)$$

where the square brakets indicate ensemble averaging over K realizations of climate evolution obtained by various models from different initial conditions and n is the time index. Steinman et al. (2015) argued that (1b) based on the multi-model ensemble mean over the 116 simulations results in the independent realizations of intrinsic variability ε. However, we show here (**Fig. 1**) using the unbiased estimate (1a) based on independent ensembles of individual model simulations (Table 1) that the "intrinsic variability" as defined by these authors is in fact dominated by the differences in the actual forced response of individual models, leading to an inflated spectrum (Figs. 1A–C) and correlated "intrinsic" samples in a given model's ensemble (Figs. 1D–F). Furthermore, using independent estimates of the forced signal from the 18 model ensembles considered to isolate the *observed* intrinsic variability demonstrates large uncertainties in the attribution of the observed climate change (Figs. 1G–I).

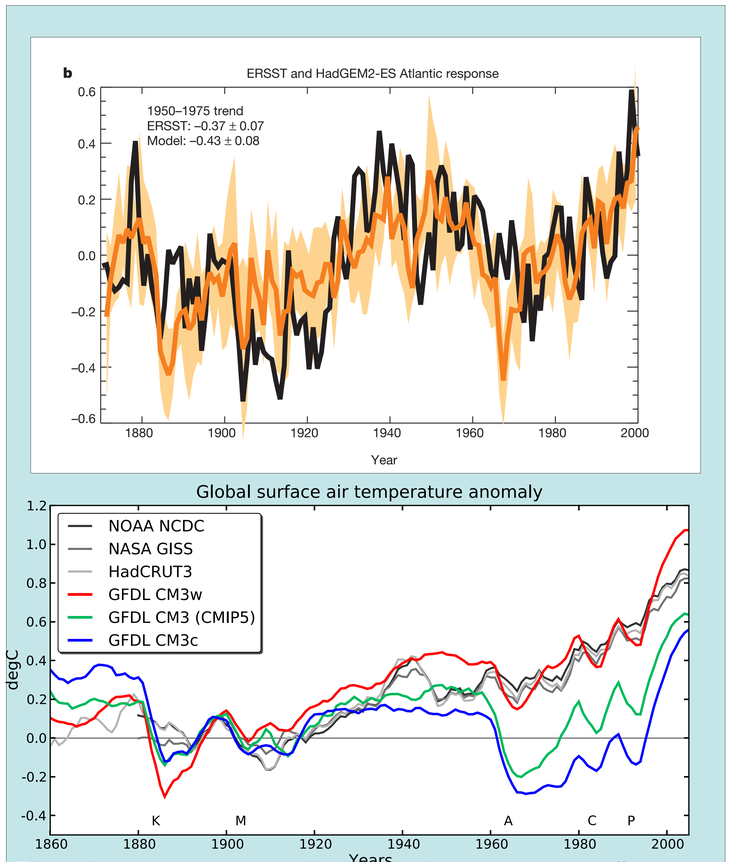

Figure 2: Twentieth-century climate simulations using two different climate models. Top: HadGEM2-ES (Booth et al. 2012) simulation of the North Atlantic sea-surface temperature (SST) evolution. Due to its treatment of the aerosol indirect effect on clouds this model is able to closely mimic the observed time series of the North Atlantic SSTs. Bottom: Three simulations (shown is the global temperature time series) using slightly different, but plausible cloud parameterizations in the GFDL CM3 model (Golaz et al. 2013). Note the pronounced differences in both the overall warming trend and multidecadal undulations of the global temperatures in the three simulations. "Model climate sensitivity can be engineered!" (Golaz and Zhao 2015)

Discussion

Finally, we would like to point out that the true simulated multidecadal intrinsic variability defined using (1a) applied to individual model ensembles is much weaker than in any of the purely empirical or semi-empirical estimates of the observed intrinsic variability in Figs. 1G–I. In particular, the standard deviation of either of the 18 individual semi-empirical time series there, that of their ensemble mean (heavy red line), as well as the standard deviations of the time series obtained by removing linear trends (heavy cyan and magenta lines) all exceed the 95th percentile of the standard deviations based on the 40-yr low-pass filtered time series of residual variability from the 116 simulations considered (shown as the distance between black dashed lines in Figs. 1G–I). On one hand, this discrepancy may reflect the uncertainty in modeling the indirect aerosol effect on climate (Booth et al. 2012; **Fig. 2** top), or the models' sensitivity to cloud parameterizations (Golaz et al. 2013; Fig. 2 bottom). In this interpretation, the more pronounced multidecadal undulations of the observed surface temperatures would be due to models' underestimating the multidecadal component of the true forced climate response, while the true intrinsic variability in observations would be consistent with the simulated intrinsic variability. Alternatively, or in addition, climate models may misrepresent some of the dynamical feedbacks hypothesized by the authors of this presentation to be responsible for the hemispheric propagation of the AMO-type multidecadal signal (Kravtsov et al. 2014; **Fig. 3**), in which case the model–data differences would reflect the lack of multidecadal intrinsic dynamics in climate models.

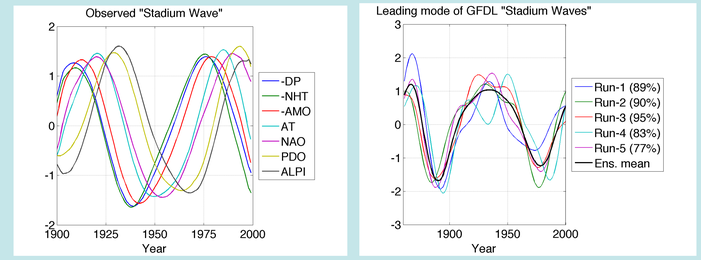

Figure 3: The results of data-adaptive spatiotemporal filtering of the multivariate climate network based on sea-surface temperature and sea-level pressure indices in the observed (left) and GFDL CM3 simulated data (right) [Kravtsov et al. 2014]. Observations are characterized by "propagation" of multidecadal "stadium wave" (Wyatt et al. 2012), whereas the simulated variability exhibits a synchronous in-phase response in all members of the simulated climate network. Furthermore, the multidecadal variance in the observed sea-level-pressure based indices is much more pronounced than in the model (not shown).

In summary, the current generation of comprehensive climate models is characterized by overwhelming model uncertainty, extreme sensitivity to aerosol and cloud parameterizations and a possible lack of multidecadal intrinsic variability, which impedes clear attribution of the twentieth century climate change.

Bibliography

Booth, B. B. B., et al., 2012. *Nature,* **484**, 228–232.

Golaz, J.-C., L. W. Horowitz & H. Levy II, 2013. *Geophys. Res. Lett.,* **40**, 2246–2251.

Kravtsov, S. & C. Spannagle, 2008. *J. Climate* **21**, 1104–1121 (2008).

Kravtsov, S., et al. 2014. *Geophys. Res. Lett.,* **41**, 6881–6888.

Steinman, B. A., M. E. Mann, & S. K. Miller, 2015. *Science*, **347**, 988–991.

Taylor, K. E., R. J. Stouffer, G. A. Meehl, 2012. *Bull. Am. Meteorol. Soc.*, **93**, 485–498.

Wyatt, M. G., S. Kravtsov, and A. A. Tsonis, 2012. *Clim. Dyn.*, **38**, 929–949.

Acknowledgements. This research was supported by the NSF grants OCE-1243158 (SK) and AGS-1408897 (SK & AAT).

For further information please contact kravtsov@uwm.edu. PDF version: https://pantherfile.uwm.edu/kravtsov/www/downloads/Marquette_Spring_2015_Kravtsov.pdf